10th World Congress on Structural and Multidisciplinary Optimization
May 19 -24, 2013, Orlando, Florida, USA

Reliability-Based Design Optimization of Highway Horizontal Curves Based on First-Order Reliability Method

Jaekwan Shin[1] and Ikjin Lee[2]

[1] University of Connecticut, Storrs, Connecticut, USA, jaekwan.shin@engr.uconn.edu
[2] University of Connecticut, Storrs, Connecticut, USA, ilee@engr.uconn.edu

1. Abstract
This paper presents reliability-based analysis and optimization of roadway minimum radius design based on vehicle dynamics, mainly focusing on exit ramps and interchanges. The performance functions are formulated as failure modes of vehicle rollover and sideslip. In order to accurately describe the failure modes, analytic models for rollover and sideslip are derived considering nonlinear characteristics of vehicle behavior using the commercial software, TruckSim. The probability of accident is evaluated using the First-Order Reliability Method (FORM) and numerical studies are conducted using a single-unit truck model. To propose practical application of the study, the reliability analysis for the minimum radius recommended by American Association of State Highway and Transportation Officials (AASHTO) is conducted. The results show that the current design method could not guarantee sufficient margin of safety against both of rollover and sideslip at low speed when there are deviations from assumed design conditions. Based on the reliability analysis, Reliability-Based Design Optimization (RBDO) is carried out and the results propose new recommendation of minimum radius satisfying target reliability level.
2. Keywords: first-order reliability method (FORM); reliability-based design optimization (RBDO); horizontal curve; roadway safety

3. Introduction
Sideslip and rollover of a ground vehicle are important road safety problems worldwide. Statistical studies have shown that a significant number of severe vehicle accidents involves sideslip and rollover [1,2]. In order to resolve this problem, ground vehicles are increasingly relying on electromechanical systems such as Anti-lock Braking System (ABS) and Electronic Stability Control (ESC) to detect and prevent hazards. According to the United States Insurance Institute for Highway Safety, ESC has reduced fatal crash involvement risk by 33% from 1999 to 2008 [3]. However, although the contribution of electronic safety systems is remarkable, that doesn't mean these systems are fundamental solution of vehicle accidents. Despite the safety systems have been widely equipped from the beginning of 2000s, the Fatality Analysis Reporting System (FARS) of the National Highway Traffic Safety Administration (NHTSA) shows that 32,885 people were still killed in 30,196 fatal crashes on the United States roadway system in 2010 [4]. This suggests that the problem cannot be resolved only by the development of the advanced vehicle systems and we should also focus on fundamental causes of the accidents.
The causes of road accidents consist of the roadway, the driver, and the vehicle. A statistical research shows that the road-environment-related factors contribute to 27% of accidents in the United States [5] and another study shows that geometric design elements are associated with 34% of crash causation in the United States and Great Britain [6]. These studies imply that poor road condition or improperly designed roads are often the causes of vehicle accidents. In particular, it should be noticed that curved roads such as exit ramps and interchanges have a much higher average accident rate in both rollover and sideslip than straight roads [7]. For this reason, providing a safe transportation system for people has received attention as one of the most important factors to enhance road safety.
American Association of State Highway and Transportation Officials (AASHTO) Green Book [8] provides design guidelines for horizontal curves, which is the design standard to determine the minimum radius for the curve to secure drivers' comfort and prevent vehicle accidents. However, several researches have pointed out the disadvantage of the current geometric design standards in terms of insufficient consideration of safety under certain circumstances and deviation from the standard requirement [9-12]. This indicates that the deterministic design method cannot provide explicit safety margin of roadway horizontal curve design, and thus probabilistic studies are required.
In the real world, more confidential results are drawn by taking uncertainty into engineering problems. For example, Kim et al. proposed numerical formulations demonstrating the realistic distribution of external reaction forces and joint actuation for the optimization of dynamical systems [13,14]. Also, Lee et al. studied the shape design of a roadarm of a tracked vehicle [15] using Reliability-Based Design Optimization (RBDO) and developed Reliability-Based Robust Design Optimization (RBRDO) model of crashworthiness for vehicle side impact [16].

The methodologies used in the engineering problems described above are basically based on numerical involvement of analytically quantified effects of uncertainty.
In the area of road geometry design, researchers also have attempted to study reliability-based safety analysis. Navin introduced the first concept of reliability-based analysis for road geometric design using the reliability index approach [17]. Chen et al. studied reliability-based assessment of vehicle safety and transient behavior of a heavy truck in adverse condition considering wind effects [18]. You et al. reported the modified model to evaluate the probability of sideslip and rollover based on the current design method recommended by AASHTO Green Book [9]. These studies show the necessity and possibility of the curve design based on reliability analysis, but they do not provide a practical and reliable design methodology under uncertainties of vehicle behavior and road condition using RBDO [19].
The main focuses of this study are classified into two parts: 1) reliability analysis of vehicle's sideslip and rollover on horizontal curves using the First-Order Reliability Analysis Method (FORM), 2) design optimization of minimum radius of horizontal curves using RBDO method. In Section 4, analytical models are developed to describe rollover and sideslip based on the existing vehicle dynamics theory. Section 5 briefly reviews FORM and derives the analytic limit state functions and their sensitivities. Section 6 illustrates results of the reliability analysis at various conditions and the minimum radius recommended by AASHTO. Furthermore, minimum radii considering vehicle safety are calculated using RBDO. Conclusions and future researches are discussed in Section 7.

4. Vehicle modeling

4.1 Review of lateral vehicle dynamics

To provide essential background knowledge for the reliability-based model, this section provides formulation of a vehicle model for lateral dynamics based on Ref. 20 and 21. At high speed cornering commonly faster than 20 km/h, since the radius of turn is much larger than the wheelbase of a vehicle, it is more convenient to analyze the dynamics of a bicycle model shown in Fig. 1 than use a four-wheel model.

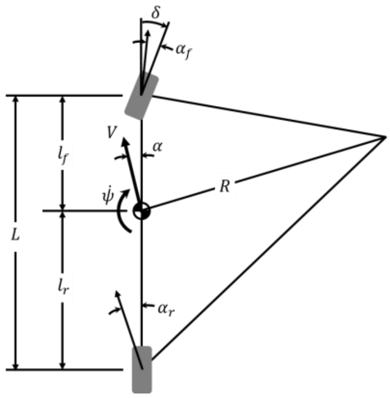

Figure 1. Vehicle model

The steer angle of the vehicle (δ) must be changed with the radius of turn (R) and/or the lateral acceleration (a_y) as

$$\delta = 57.4\frac{L}{R} + \alpha_f - \alpha_r = \frac{R}{L} + Ka_y \tag{1}$$

where L is the wheelbase of the vehicle, K is the understeer gradient, α_f and α_r are the side slip angle of the front and rear tires respectively. R is given by

$$R = \frac{57.3Lg + KV^2}{g\delta} \tag{2}$$

where g is the gravitational acceleration, V is the speed of the vehicle at the center of gravity (c.g.).
Based on the bicycle model, yaw velocity ($\dot{\psi}$) and sideslip angle (α) of the vehicle at c.g., which are useful characteristics to understand and analyze lateral dynamics, are derived as

$$\dot{\psi} = \frac{V}{R} \tag{3}$$

and

$$\alpha = 57.3\frac{l_r}{R} - \frac{W_r V^2}{C_{\alpha r} g R} \tag{4}$$

respectively, where W_r is the vertical load on the rear axle and $C_{\alpha r}$ is the cornering stiffness of rear tires.

4.2 Rollover

Figure 2 shows the rear view of a vehicle in cornering. The roll angle (ϕ) of the sprung mass can be derived using moment equilibrium about the roll axis as [20,21]

$$\phi = \frac{m_s g\left(h_{cg} - h_r\right)V^2}{\left(K_{\phi f} + K_{\phi r} - m_s g\left(h_{cg} - h_r\right)\right)Rg} \tag{5}$$

where m_s is the sprung mass of the vehicle, h_{cg} and h_r are the height of the center of gravity of the sprung mass and the height of the roll center, and $K_{\phi f}$ and $K_{\phi r}$ are the roll stiffness of the front axle and the rear axle, respectively.

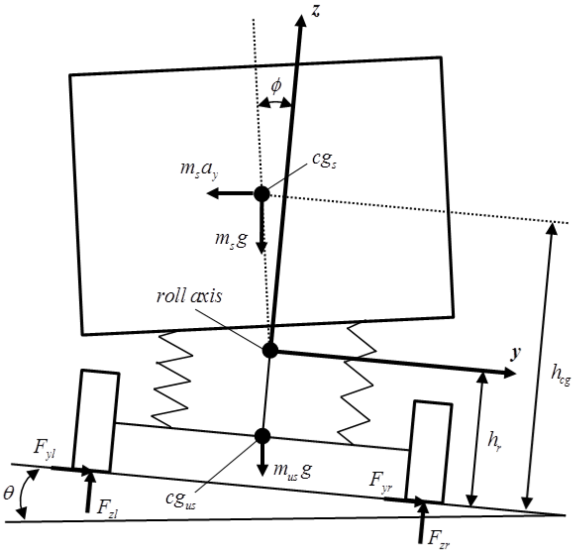

Figure 2. Vehicle model (rear view)

If all wheels of one side of the vehicle are lifted up, there is no reaction force on the side, and it can be concluded that the vehicle rolls over. In other words, rollover occurs when the transferred weight between one side and the other side is larger than a half of the vehicle weight. Thus, the criterion of rollover is derived as [22,23]

$$W_{trans} = \frac{h_{cg} m}{l_w}\left[V\left(\dot{\alpha} + \dot{\psi}\right) + g\left(\phi - \theta\right)\right] > \frac{mg}{2} \tag{6}$$

where W_{trans} is the transferred weight and θ is the road bank angle.

4.3 Sideslip

The criteria of sideslip are classified as sideslip of all wheels, the front axle, or the rear axle. In this study, sideslip of one axle is considered as the criterion of sideslip because sideslip of all wheels eventually are caused by sideslip of one axle. For instance, when considering a vehicle whose center of gravity is closer to the rear axle than the front axle in longitudinal direction, it is enough to observe only sideslip of a front axle because the front tires generate larger side friction forces than the rear tires in steady state cornering. The vehicle will start to slip when the total lateral tire forces on the front axle exceed allowable friction force that is determined by the road-tire friction coefficient (C_f) and the weight of the vehicle. This relationship can be described as [24]

$$F_{yf} = C_{\alpha f}\alpha_f > C_f W_f + W_f \sin\theta \tag{7}$$

where F_{yf} is the lateral tire force of the front axle and W_f is the vertical force on the front axle. The side slip angle of the front axle, α_f, can be derived as [20,21]

$$\alpha_f = \delta - \alpha - \frac{l_f\dot{\psi}}{V_x} \tag{8}$$

where V_x is the longitudinal speed of the vehicle.

4.4 Simplification of the nonlinear characteristics of vehicle behavior

Forces acting on each tire highly influence the dynamic behavior of a vehicle. For given tires, the cornering characteristic of a vehicle is mainly dependent on the vertical load and cornering stiffness. Figure 3 shows a graph of the lateral tire force for a typical truck tire in the TruckSim, which is commercial software to simulate dynamics of heavy trucks in high fidelity and is widely used in the area of vehicle dynamics and control. In general, tire forces can be expressed by a function of lateral force and vertical load, and Dugoff's tire model and Pacjeka's magic formula are widely used [21]. However, these mathematical models cannot be applied in this study because they estimate longitudinal and lateral tire forces at given vertical load and side slip but the vertical load is unknown in this study. For this reason, we adopt a method to directly use understeer gradient that is the most widely used characteristic to express vehicle's cornering behavior.

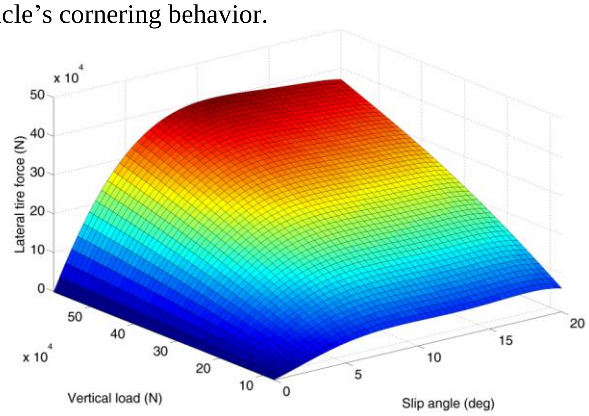

Figure 3. Tire curve - Source: TruckSim

To derive a simple lateral tire model, it can be assumed that the camber thrust is ignorable, which is a lateral force produced by the inclination of a wheel outward from the body. Hence, when a vehicle is cornering, the lateral tire forces are approximated to be proportional to the tire slip angle as

$$F_{yi} = C_{\alpha i}\alpha_i \tag{9}$$

where $C_{\alpha i}$ represents lateral tire stiffness and α_i is tire sideslip angle. The subscript i indicates the front and rear axle, respectively. This simple tire model can describe tire force very properly before the beginning of sideslip and it has been widely used and verified in the field of vehicle dynamics and control [23-26].

According to Eq. (1), the understeer gradient determines the magnitude and direction of the steering inputs required and is given by

$$K = \frac{W_f}{C_{\alpha f}} - \frac{W_r}{C_{\alpha r}} \tag{10}$$

where W_f is the vertical load on the front axle, and $C_{\alpha f}$ and $C_{\alpha r}$ are the cornering stiffness of the front and rear tires, respectively. By the assumption that the cornering stiffness of tire is constant as derived in Eq. (9), the understeer gradient can be calculated using Eq. (10) and it has also constant value. In this study, we define the constant understeer gradient for sideslip as K_s which is 2.5322.

In contrast, in the case of rollover the simple tire model could not be justified anymore due to nonlinear characteristics of vehicle behavior that is mainly caused by tires shown in Fig. 3. Since there is large weight transfer when rollover occurs, the lateral tire forces could not be approximated to be proportional to the tire slip angle. In order to deal with the effect of the weight transfer, an additional quadratic equation term into Eq. (1) has been used in vehicle simulation studies [22,23,27]. However, in fact, since the quadratic term approximates tire characteristic in all operating ranges, though this method would be feasible for the use of analysis in all operating ranges, it could cause large discrepancy between mathematical model and actual vehicle dynamics at the time of rollover due to its excessive simplification. Eventually, this could cause inaccurate evaluation for reliability of rollover.

In this study, an alternative approach is proposed using an equation based on a look-up table, which is one of the commonly used methods to analyze dynamic behavior of a vehicle in the area of vehicle stability controls [28]. We noticed that, to accurately estimate the probability of rollover, it is most important to know the values of understeer gradient at the time of rollover. Since the criterion of failure depends on the sign of the performance function, knowing accurate values of understeer gradient at the time of rollover means that an exact criterion of rollover is available. In other word, if we have the accurate values of understeer gradient at the time of rollover, we could considerably enhance accuracy of probability of failure.

The values of the understeer gradient are directly collected by co-simulation of TruckSim and Matlab/Simulink that is described in Fig. 4. Table 1 shows the obtained values of the understeer gradient at the moment of wheels being lifted up.

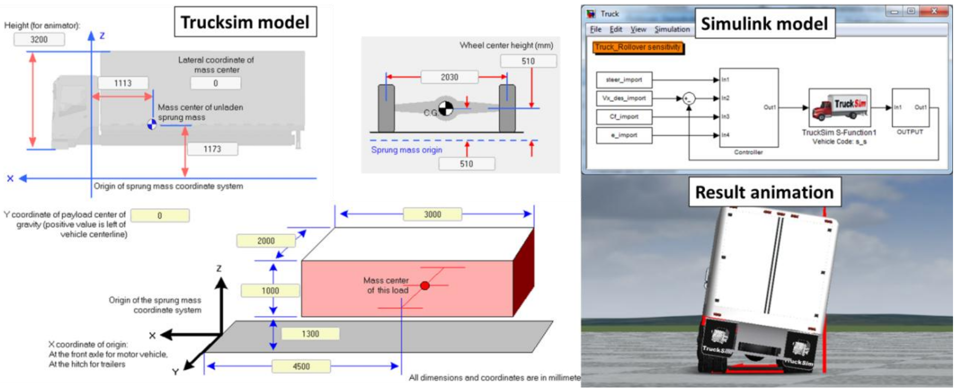

Figure 4. Co-simulation of TruckSim and Simulink

Table 1. Understeer gradient

Speed, V (km/h)	Steer angle, $\delta(°)$	Understeer gradient, K (deg/g)
30	24.48	6.55
40	14.24	4.49
50	9.62	3.98
60	7.16	3.74
70	5.69	3.61
80	4.75	3.55
90	4.11	3.50
100	3.73	3.40

Based on the data in Table 1, the understeer gradient can be formulated as a function of the speed and the steer angle as

$$K_r(V,\delta) = p_{00} + p_{10}V + p_{01}\delta \tag{11}$$

where $p_{00} = 2.5322$, $p_{10} = 0.0030$, and $p_{01} = 0.1536$. The p_{00} is the same with K_s which was calculated from

Eq. (10). Consequently, Eq. (11) consists of K_s and the effect of vehicle speed and steer angle on handling behavior, and this means that the proposed method can handle the nonlinearities in the aspect of the relationship between driver's command and vehicle's dynamic behavior.

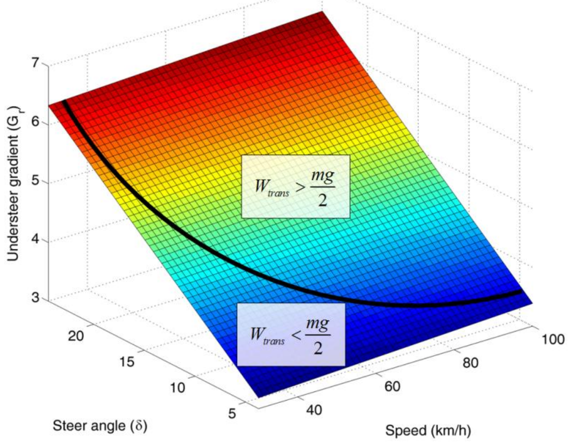

Figure 5. Understeer gradient

The understeer gradient calculated using Eq. (11) shows a plane described in Fig. 5. The obtained values of understeer gradient in Table 1 are closely positioned to the curve and this presents that a vehicle is at the moment of wheels being lifted up ($W_{trans} = mg/2$). Based on the curve, the plane is divided into two areas: $W_{trans} > mg/2$ and $W_{trans} < mg/2$.

To verify the technique above, the transferred weight of each vehicle model is compared and the result is shown in Fig. 6. When K_s is used for rollover analysis, there exists large discrepancies, which is about from 5000N at 50 km/h to 10000N at 100 km/h, compared with the result of Trucksim. On the other hand, the accuracy can be significantly enhanced when using K_r for calculating the weight transfer at the beginning of rollover although there are slight errors compared with the reference line in Fig. 6.

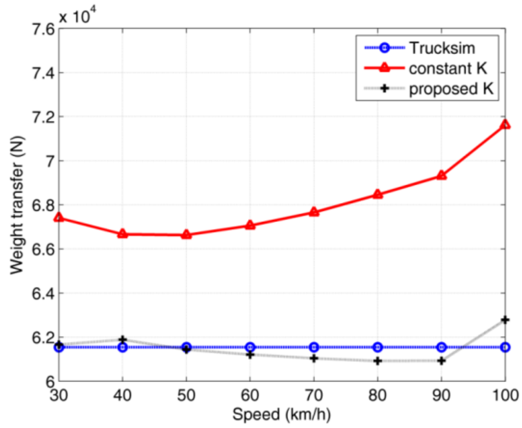

Figure 6. Transferred weight of each model

5. Reliability analysis and RBDO

5.1 Review of First-Order Reliability Method (FORM)

A reliability analysis entails calculation of probability of failure, denoted as P_F, which is defined using a multi-dimensional integral [29,30]

$$P_F \equiv P[G(\mathbf{X}) > 0] = \int_{G(\mathbf{X})>0} f_{\mathbf{X}}(\mathbf{x}) d\mathbf{x} \tag{12}$$

where $P[\bullet]$ is a probability function, $\mathbf{X}=\{X_1, X_2, \cdots, X_N\}^{\mathrm{T}}$ is an N-dimensional random vector where the upper case X_i means that they are random variables and the lower case x_i means that they are the realization of the random variable X_i, $G(\mathbf{X})$ is the performance function such that $G(\mathbf{X})>0$ is defined as failure, and $f_{\mathbf{X}}(\mathbf{x})$ is a joint Probability Density Function (PDF) of the random variable $\mathbf{X}$. For the computation of the probability of failure in Eq. (12), FORM linearizes $G(\mathbf{X})$ at the Most Probable Point (MPP) in U-space obtained through Rosenblatt transformation and the linearized function is given by

$$G(\mathbf{X})=g(\mathbf{U})\cong g_L(\mathbf{U})=g(\mathbf{u}^*)+\nabla g^{\mathrm{T}}(\mathbf{U}-\mathbf{u}^*) \tag{13}$$

where $\mathbf{u}^*$ is the MPP in U-space which is defined as the point on the limit state function with minimum distance from the origin, and is obtained by solving the following optimization to

$$\begin{aligned} &\text{minimize} && \|\mathbf{u}\| \\ &\text{subject to} && g(\mathbf{u})=0 \end{aligned} \tag{14}$$

and ∇g is the gradient vector of the performance function evaluated at the MPP in U-space. Using the definition of the MPP, Eq. (13) is further simplified as

$$g_L(\mathbf{U})=\nabla g^{\mathrm{T}}(\mathbf{U}-\mathbf{u}^*) \tag{15}$$

since $g(\mathbf{u}^*)=0.$ The reliability index, denoted as β, is then defined as the distance from the origin to $\mathbf{u}^*$ and is given by [31]

$$\beta=\|\mathbf{u}^*\|=\left(\mathbf{u}^{*\mathrm{T}}\mathbf{u}^*\right)^{1/2} \tag{16}$$

Using the linearized performance function and the reliability index β, FORM approximates the probability of failure in Eq. (12) as

$$P_F^{\mathrm{FORM}}\cong\Phi(-\beta) \tag{17}$$

where $\Phi(\bullet)$ is the standard normal Cumulative Distribution Function (CDF).

5.2 Review of Reliability-Based Design Optimization (RBDO)

The mathematical formulation of RBDO is expressed as

$$\begin{aligned} &\text{minimize} && \mathrm{cost}(\mathbf{d}) \\ &\text{subject to} && P\left[G_j\left(\mathbf{X}\right)>0\right]\le P_{F_j}^{\mathrm{tar}}, \quad j=1,\dots,\mathrm{NC} \\ & && \mathbf{d}^{\mathrm{L}}\le\mathbf{d}\le\mathbf{d}^{\mathrm{U}}, \quad \mathbf{d}\in\mathbf{R}^{\mathrm{ndv}}, \text{ and } \mathbf{X}\in\mathbf{R}^{N} \end{aligned} \tag{18}$$

where $\mathbf{d}=\boldsymbol{\mu}(\mathbf{X})$ is the design vector, which is the mean value of the N-dimensional random vector $\mathbf{X}=\left\{X_1,X_2,\dots X_N\right\}^{\mathrm{T}}$, $P_{F_j}^{\mathrm{tar}}$ is the target probability of failure for the j^{th} constraint; and NC, ndv, and N are the number of probabilistic constraints, design variables, and random variables, respectively [32].
To carry out RBDO using Eq. (18), the probabilistic constraints and their sensitivities must be evaluated, which are derived in Section 5.3 and Section 5.4, respectively.

5.3 Performance function

Researchers have investigated the probabilistic characteristics of design variables such as vehicle mass, radius, friction coefficient, deceleration rate, brake reaction time, and wind speed which can affect roadway safety [12,13,33]. In this study, speed of a vehicle, steer angle of the front wheels, tire-road friction coefficient, and road bank angle are selected as input random parameters. This can be written formally as

$$\mathbf{X} = \left\{V\ \delta, C_f, \theta\right\}^T \tag{19}$$

The limit state of performance can be defined in terms of loss of stability. The present study utilizes the following criteria: rollover and sideslip of all four wheels. Thus, the limit state function for rollover is given by

$$G_r(\mathbf{X}) = \frac{h_{cg} m}{l_w}\left[V\left(\dot{\alpha}(\mathbf{X}) + \dot{\psi}(\mathbf{X})\right) + g\left(\phi(\mathbf{X}) - \theta\right)\right] - \frac{mg}{2} \tag{20}$$

and the limit state function for sideslip is given by

$$G_s(\mathbf{X}) = C_{\alpha f}\alpha_f(\mathbf{X}) - C_f W_f - W_f \sin\theta \tag{21}$$

5.4 Sensitivity of performance function

In order to apply FORM, the gradient vector of the performance functions, which called sensitivities, is required in Eq. (15). A Finite Difference Method (FDM) could be used for the sensitivity calculation. However, the FDM is inefficient due to additional functional evaluations and may fail to get accurate sensitivities according to nonlinearity of performance functions. In this study, analytic forms of sensitivities are straightforwardly derived. This can make not only overall process computationally efficient, but also sensitivities accurate. Sections 5.4.1 and 5.4.2 explain how to derive sensitivities of the two performance functions.

5.4.1 Sensitivity of rollover

$$\frac{dG_r(\mathbf{X})}{dV} = \frac{h_{cg} m}{d}\left[\dot{\psi}(\mathbf{X}) + V\frac{d\dot{\psi}(\mathbf{X})}{dV} + g\frac{d\phi(\mathbf{X})}{dV}\right] \tag{22}$$

and it is straightforward to obtain the derivative terms in the right side using Eqs. (2), (3), (5), and (11). In a similar manner, the sensitivities of rollover with respect to steer angle, road friction coefficient, and road bank angle are derived as

$$\frac{dG_r(\mathbf{X})}{d\delta} = \frac{h_{cg} m}{d}\left[V\frac{d\dot{\psi}(\mathbf{X})}{d\delta} + g\frac{d\phi(\mathbf{X})}{d\delta}\right], \tag{23}$$

$$\frac{dG_r(\mathbf{X})}{dC_f} = 0, \tag{24}$$

and

$$\frac{dG_r(\mathbf{X})}{d\theta} = -\frac{h_{cg} m}{l_w} g\ . \tag{25}$$

The derivative terms in the right side in Eq. (22) are obtained using Eqs. (2), (3), (5), and (11).

5.4.2 Sensitivity of sideslip

Likewise, the sensitivities for sideslip can be derived as derivatives of Eq. (21) with respect of each random variable as

$$\frac{dG_s(\mathbf{X})}{dV} = \frac{d\alpha_f(\mathbf{X})}{dV}, \tag{26}$$

$$\frac{dG_s(\mathbf{X})}{d\delta} = \frac{d\alpha_f(\mathbf{X})}{d\delta}, \tag{27}$$

$$\frac{dG_s(\mathbf{X})}{dC_f} = -W_f, \tag{28}$$

and

$$\frac{dG_s(\mathbf{X})}{d\theta} = W_f \cos\theta\ . \tag{29}$$

Again, it is straightforward to obtain the derivative terms in the right side of Eqs. (26) and (27) using Eqs. (2), (3), (4), and (8).

6. Numerical study

In this section, probabilities of failure modes of a heavy truck are evaluated based on the analytic models derived in the previous sections. First, the reliability analysis is conducted at various conditions of the random variables to verify the developed model in Sections 4 and 5. Second, in order to propose a practical application of this study, the reliability analysis for the minimum radius recommended by AASHTO at various speeds and bank angles is conducted. In addition, new minimum radii are designed using RBDO. In this study, all random variables are assumed to be normally distributed.

6.1 Vehicle parameters

A single-body heavy truck model is used in this study because in general a truck is more vulnerable to rollover than a passenger car. All of the parameters are listed in Table 2 and obtained from a conventional van 5.5T/8.5T model in Trucksim which is described in Fig. 7.

Figure 7. Conventional van 5.5T/8.5T model in TruckSim

Table 2. Parameters of the truck model

Parameter	Value
Total mass, m	12551 kg
Sprung mass, m_s	11246 kg
Unsprung mass, m_{us}	1305 kg
Longitudinal distance from c.g. to front tires, l_f	3.1346 m
Longitudinal distance from c.g. to rear tires, l_r	1.885 m
Distance between left and right wheels, l_w	2.03 m
Height of the c.g. of vehicle from road, h_{cg}	1.3933 m
Height of the roll center from road, h_r	0.51 m
Cornering stiffness of the front tires, $C_{\alpha f}$	4700.3 N/deg
Cornering stiffness of the rear tires, $C_{\alpha r}$	10527 N/deg
Roll stiffness of the front suspension, $K_{\phi f}$	5.74e+07 Nm/deg
Roll stiffness of the rear suspension, $K_{\phi r}$	8.76e+07 Nm/deg

6.2 Case study at various conditions

Numerical studies are carried out in this section at various conditions of the random variables to verify the developed model in Sections 4 and 5. Using FORM and limit state functions given in Eqs. (20) and (21), probabilities of rollover and sideslip are calculated, respectively. The standard deviations of the random variables are selected or assumed based on the existing studies [14,34,35] and given in Table 3. Road bank angle, denoted by θ, is converted to the percentage value, denoted by e, as

$$e = \tan\theta \tag{30}$$

which is called a superelevation in the AASHTO Green Book. Test conditions are listed in Table 4. The tire-road friction coefficient can provide conditions of pavement listed in Table 5 [36].

Table 3. Standard deviations of random variables

Variable	Standard deviation
Speed, V	0.15 μ_V
Tire Steer Angle, δ	0.1 μ_δ
Tire-Road Friction Coefficient, C_f	0.05
Road bank angle, θ	0.1 μ_θ

Table 4. Test scenarios

	Speed, μ_V (km/h)	Tire Steer Angle, μ_δ (deg)	Tire-Road Friction Coefficient, μ_{C_f}	Superelevation, μ_e (%)
Case 1	50 - 80	5	0.8	0
Case 2	80	3 - 6	0.8	0
Case 3	70	5	0.2 - 0.8	0
Case 4	70	5	0.4	0 - 8

Table 5. Tire-road friction coefficient

Road conditions	C_f
Dry asphalt	0.8
Wet asphalt	0.6
Snow	0.3
Ice	0.1

Figure 8 gives the results of probabilities of rollover and sideslip under varying mean speeds (Case 1). Although the probabilities of rollover and sideslip are considerably low at 50 km/h, the probabilities increase as the vehicle speed increases. Compared with the probability of sideslip, the probability of rollover is much more influenced by the vehicle speed. The above result corresponds well with the previous research that a truck is more likely to roll over than skid on a dry road [9,24,37], and the same conclusion is drawn in terms of the reliability analysis in this study. Also, this result implies that the maximum speed limit is significant for preventing rollover accident on curves.

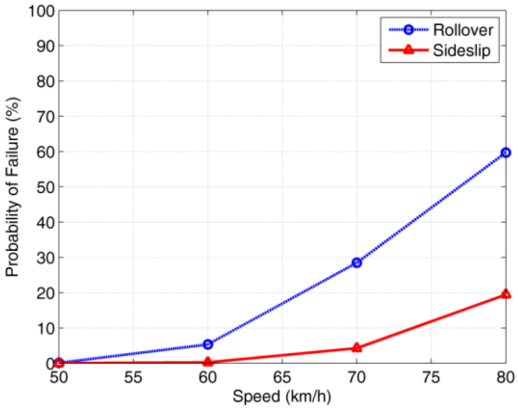

Figure 8. Probability of failure versus speed

Figure 9 shows the results of probabilities of rollover and sideslip at various steer angles (Case 2). The probability of failure gradually increases as steer angle increases. This result is analogous to the result of the probability of failure at various speeds described in Fig. 8 and also agrees with previous studies [9,24,37]. In addition, the results at various steer angles suggest that a regulation for the radius of curved roads is required to prevent rollover and sideslip. For this reason, the minimum radius of curved roads is recommended by the AASHTO Green book.

Figure 10 gives the results of the probabilities of rollover and sideslip under different tire-road friction coefficients (Case 3). The result shows that the probability of sideslip drastically decreases as the friction coefficient increases. On the other hand, the probability of rollover is not influenced by the road condition and is higher than that of sideslip on dry road. This result agrees with the existing researches [9,36] which criticize that the minimum radius design recommended by AASHTO ignores the rollover only focusing on the sideslip. Also, this indicates that rollover has to be more significantly considered than sideslip at a high friction coefficient, that is dry road condition, and it is required to develop a new design method to cover all aspects of hazards.

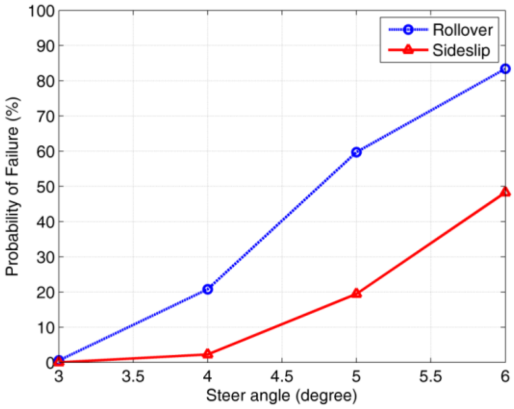

Figure 9. Probability of failure versus steer angle

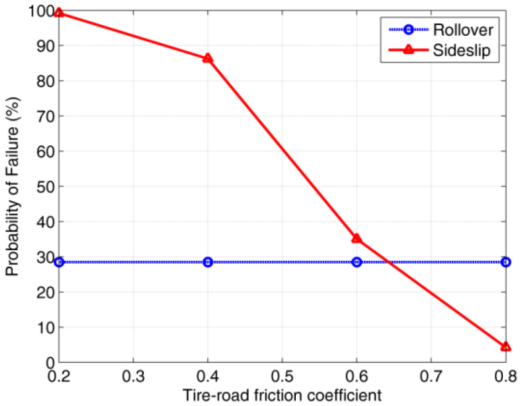

Figure 10. Probability of failure versus tire-road friction coefficient

Figure 11 shows the result of the probabilities of rollover and sideslip under different super-elevations (Case 4). The results indicate that the superelevation contributes to reducing both rollover and sideslip. This means that increasing road bank angle is an effective way to prevent rollover and sideslip of vehicles driving on a curved road and it is the reason why exits or ramps of highways have slight superelevations. However, though the superelevation is helpful, it is not highly significant to reduce road accidents on curves and this result is in accord with the result of the existing studies [9,24,37].

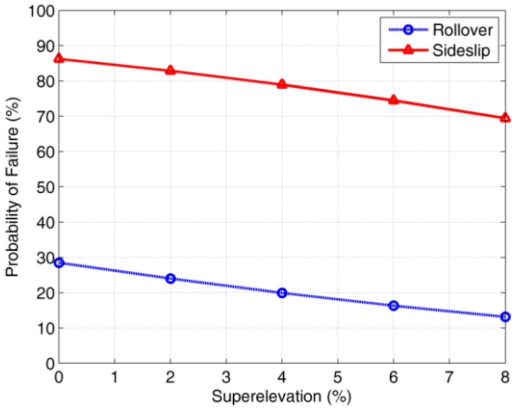

Figure 11. Probability of failure versus superelevation

6.3 Reliability analysis for the minimum radius recommended by AASHTO

To propose practical application of this study, this section investigates the probabilities of rollover and sideslip for the minimum radius guided by the AASHTO Green Book, mainly focusing on exit ramps and interchanges.

According to the Green Book, the minimum radius ($R_{\min}$) at given speeds, friction, and superelevations can be determined directly from

$$R_{\min} = \frac{V^2}{127\left(e + f_{\max}\right)} \tag{31}$$

where $f_{\max}$ is the maximum side friction demand defined in the Green Book which indicates that the required side force for driving on the roads with the minimum radii. To be compatible with the developed analytic model in this study, the mean steer angles in Table 6 are obtained from Eq. (2) based on the given speeds and recommended radii. Road condition is chosen as wet because the current design criterion intends to maintain the vehicle's lateral acceleration within driver comfort levels that are below the lateral acceleration at which the vehicle would skid on a wet road [35].

In Eq. (31), V is design speed indicating the maximum safe speed on the road with minimum geometric elements applied. What's more, a statistical study shows a high correlation of mean speed of vehicles with radii of roads [38]. Thus, based on this existing study, mean speeds and standard deviations on each horizontal curve with different minimum radii are calculated as

$$\mu_V = 14.75 \ln R_{\min} - 11.69 \tag{32}$$

and

$$\sigma_V = 0.1085 \mu_V + 0.99 \tag{33}$$

respectively, where $R_{\min}$ is the minimum radius in the Green Book, μ_V is the mean of vehicle speed and σ_V is the standard deviation of vehicle speed.

Table 6 shows minimum radii recommended by the AASHTO Green Book and corresponding probabilities of rollover and sideslip under wet road condition. The probabilities of rollover and sideslip at 30km/h are significantly higher than those at 50km/h. This result is due to the higher maximum friction demand for 30km/h used in the current design method.

Table 6. Minimum radius recommended by AASHTO and corresponding probability of failure

Speed, V (km/h)			Maximum friction demand, $f_{\max}$ (g)	Super-elevation, e (%)	Minimum radius, $R_{\min}$ (m)	Steer angle, δ (deg)		Probability of failure (%)	
Design	Mean*	SD**				Rollover	Sideslip	Rollover	Sideslip
30	33.9	4.67	0.28	4	22	15.09	14.11	11.93	8.87
30	33.22	4.59	0.28	6	21	15.76	14.74	10.31	7.42
30	32.5	4.52	0.28	8	20	16.51	15.43	8.96	6.21
30	31.74	4.43	0.28	10	19	17.33	16.19	7.67	5.12
30	30.94	4.35	0.28	12	18	18.23	17.03	6.55	4.23
50	54.01	6.85	0.19	4	86	4.24	4.02	0.0017	0.0083
50	52.76	6.71	0.19	6	79	4.58	4.34	0.0030	0.010
50	51.59	6.59	0.19	8	73	4.92	4.67	0.0046	0.012
50	50.55	6.47	0.19	10	68	5.26	4.98	0.0065	0.013
50	49.65	6.38	0.19	12	64	5.56	5.26	0.0077	0.012

* Using Eq. (32).

** SD stands for standard deviation. Using Eq. (33).

The high probabilities of rollover and sideslip can be explained by the concept of the margin of safety and thus it is possible to explain the higher probability of sideslip at 30km/h by using the concept of the friction margin. The maximum friction demands are 0.28g at 30km/h and 0.19g at 50km/h. In case of a truck, the maximum friction demand is 10% higher than for a passenger car. Thus, the maximum friction demands are calculated as 0.31g at 30km/h and 0.21g at 50km/h [36]. Based on the current design method, the margin of safety against sideslip can be calculated as the differences between the available friction and the maximum friction demand. Thus, the margin of safety against sideslip under wet condition is calculated as

$$0.60g - 0.31g = 0.29g \tag{34}$$

This indicates that if the magnitude of additional side force caused by the effect of the random variables is larger than 0.29g, sideslip occurs at 30km/h on wet roads. In contrast, since the safety margin against sideslip is 0.39g at 50km/h, the probability of sideslip at 50km/h is significantly low. Similarly, the higher probability of rollover can be explained using the concept of rollover threshold and the margin of lateral force against rollover, which is basically the same concept with the margin of friction described above.

Consequently, this result implies that the current design method cannot provide the sufficient margin of safety against both rollover and sideslip when there are deviations from assumed conditions, especially at low speed. Thus, the potential safety problem created by deviations from the design assumptions should be dealt with in terms of reliability. This implies that the Reliability-Based Design Optimization (RBDO) is necessarily required.

6.4 Reliability-based minimum radius optimization

Given speed limit, road friction coefficient, and superelevation, the RBDO problem for the minimum radius is formulated to

$$\begin{aligned} &\text{minimize} && R(d) \\ &\text{subject to} && P\left[G_j(\mathbf{X}) > 0\right] \le P_{F_j}^{\text{tar}}, \quad j = r, s \\ & && 0 \le d \le 20, \quad d \in \mathbf{R}^1, \text{ and } \mathbf{X} \in \mathbf{R}^4 \end{aligned} \tag{35}$$

where d is the mean of the steer angle (δ) and $P_F^{\text{tar}} = \Phi^{-1}(-\beta_t)$ that is called the target probability of failure. β_t is the target reliability index and set up to be 3 ($P_F^{\text{tar}} = 0.1350\%$), 3.5 ($P_F^{\text{tar}} = 0.02326\%$), and 4 ($P_F^{\text{tar}} = 0.003167\%$). V, C_f, and θ are random parameters and δ is only a random variable in the RBDO problem. Since the mathematical models to evaluate rollover and sideslip are independently derived in terms of understeer gradient, the RBDO problem should be separately dealt with. Hence, the minimum radius is chosen as a larger one between results of the two performance functions.

The RBDO results are shown in Table 7. At 30km/h of the design speed, the minimum radius obtained using RBDO is larger than the recommended radius by AASHTO in all target reliabilities. Especially when the target reliability is 4 at 30km/h, RBDO results show 1.6~1.7 times larger than the radii of AASHTO. In contrast, at 50km/h design speed, RBDO results in similar level of radii when the target reliability is 3.5 or 4, and the increased magnitude of radii are not significant compared with the case of 30km/h when the target reliability is 4. These are reasonable results compared with the results of reliability analysis in Table 6. In conclusion, while the current design method does not consider rollover and is also not systematic in terms of probabilistic engineering, the proposed RBDO method can comprehensively treat the minimum radius design considering probability of accidents and the target reliability.

Table 7. Minimum radius design using RBDO

Speed, V (km/h)			Maximum friction demand, $f_{\max}$ (g)	Super-elevation, e (%)	Minimum radius design, $R_{\min}$ (m)			
Design	Mean*	SD**			AASHTO	RBDO		
						$\beta_t = 3$	$\beta_t = 3.5$	$\beta_t = 4$
30	33.9	4.67	0.28	4	22	32.17	35.78	39.60
30	33.22	4.59	0.28	6	21	30.00	33.35	36.91
30	32.5	4.52	0.28	8	20	28.02	31.06	34.37
30	31.74	4.43	0.28	10	19	26.19	28.87	31.95
30	30.94	4.35	0.28	12	18	24.42	26.81	29.64
50	54.01	6.85	0.19	4	86	74.32	81.62	89.53
50	52.76	6.71	0.19	6	79	68.91	75.66	82.99
50	51.59	6.59	0.19	8	73	64.10	70.38	77.20
50	50.55	6.47	0.19	10	68	59.93	65.80	72.17
50	49.65	6.38	0.19	12	64	56.69	61.86	67.84

* Using Eq. (32).
** SD stands for standard deviation. Using Eq. (33).

7. Conclusions

This paper presents Reliability-Based Design Optimization (RBDO) of minimum radius of roadway horizontal curves using the first-order reliability analysis of rollover and sideslip. Two analytic models for the reliability analysis are developed considering the nonlinear characteristic of vehicle behavior. The results of the numerical study at various conditions show that rollover is highly sensitive to vehicle speed and steer angle, on the other hand, sideslip is vulnerable to the change of tire-road friction coefficient. In addition, the probabilities of both accidents can be decreased by superelevation. The results of reliability analysis of the minimum radii recommended by the AASHTO Green Book implies that it is necessary to consider rollover prevention and deviation from design condition in designing roadway curves. Based on the reliability analysis, RBDO are carried out and the results propose new recommendations of minimum radii satisfying target reliability levels.

Future researches may be explored in the following directions. First, a vehicle model should be selected to represent all vehicles on roads. This is brought up because this study is based on mathematical modeling of a vehicle. Although the Green Book provides general classes of design vehicles, it does not define detailed parameters of the vehicles. Second, it would be desirable to consider wind effects since the probability of accident would be higher in a high cross wind. Finally, Second-Order Reliability Method (SORM) or a more accurate method would be applied to enhance accuracy of reliability analysis.

8. References

[1] Strashny, A., An analysis of motor vehicle rollover crashes and injury outcomes, NHTSA's National Center for Statistics and Analysis, HS-810 741, Transportation Research Board, 2007.

[2] MacLennan, P. A., Marshall, T., Griffin, R., Purcell, M., McGwin, G., and Rue, L. W., Vehicle rollover risk and electronic stability control systems, *Injury Prevention*, 14(3),154-158, 2008.

[3] Farmer, C. M., Effects of electronic stability control on fatal crash risk, Insurance Institute for Highway Safety, 2010.

[4] NHTSA Fatality Analysis Reporting System (FARS) Encyclopedia, Available: http://www.nhtsa.gov/FARS.

[5] Sayed, T., Abdelwahab, W., and Navin, F., Identifying accident-prone locations using fuzzy pattern recognition, *Journal of Transportation Engineering*, 121(4), 352-358, 1995.

[6] Rumar, K., The role of perceptual and cognitive filters in observed behavior, *Human behavior and traffic safety*, pp. 151-170, Springer US, 1986.

[7] Glennon, J. C., Neuman, T. R., & Leisch, J. E., Safety and operational considerations for design of rural highway curves, Federal Highway Administration, FHWA/RD-86/035, Washington, DC, 1985.

[8] American Association of State Highway, and Transportation Officials, *A policy on geometric design of highways and streets*, AASHTO, Washington, DC, 2011.

[9] You, K., Sun, L., and Gu, W., Reliability-Based Risk Analysis of Roadway Horizontal Curves, *Journal of Transportation Engineering*, 138(8), 1071–1081, 2012.

[10] Harwood, D. W., and Mason, J. M., Horizontal curve design for passenger cars and trucks, *Transportation Research Record: Journal of the Transportation Research Board*, 1445, 22-23, 1994.

[11] Ismail, K., & Sayed, T., Risk-Based Highway Design, *Transportation Research Record: Journal of the Transportation Research Board*, 2195, 3-13, 2010.

[12] Echaveguren, T., Bustos, M., and De Solminihac, H., Assessment of horizontal curves of an existing road using reliability concepts, *Canadian Journal of Civil Engineering*, 32(6), 1030-1038, 2005.

[13] Kim, J.H., Abdel-Malek, K., Xiang, Y., Yang, J., and Arora, J.S., Concurrent motion planning and reaction load distribution for redundant dynamic systems under external holonomic constraints, *International Journal for Numerical Methods in Engineering*, 88(1), 47-65, 2011.

[14] Kim, J.H. and Joo, C.B., Optimal motion planning of redundant manipulators with controlled task infeasibility, *Mechanism and Machine Theory*, 64, 155-174, 2013.

[15] Lee, I., Choi, K.K., Du, L., and Gorsich, D., Inverse Analysis Method Using MPP-Based Dimension Reduction for Reliability-Based Design Optimization of Nonlinear and Multi-Dimensional Systems, *Computer Methods in Applied Mechanics and Engineering*, 198(1), 14-27, 2008.

[16] I. Lee, K.K. Choi, L. Du, D. Gorsich, Dimension reduction method for reliabilitybased robust design optimization, *Computers & Structures*, 86(13–14), 1550-1562, 2008.

[17] Navin, F. P. D., Reliability indices for road geometric design, *Canadian Journal of Civil Engineering*, 19(5), 760-766, 1992.

[18] Chen, F., and Chen, S., Reliability-based assessment of vehicle safety in adverse driving conditions, *Transportation Research Part C: Emerging Technologies*, 19(1), 156-168, 2011.

[19] Tu, J., Choi, K. K., and Park, Y. H., A new study on reliability-based design optimization, *Journal of Mechanical Design*, 121(4), 557-564,1999.

[20] Gillespie, T., *Fundamentals of vehicle Dynamics*, SAE, 1992.

[21] Rajamani, R., *Vehicle dynamics and control*, Springer, 2011.

[22] Sampson, D. J., and Cebon, D., Active roll control of single unit heavy road vehicles, *Vehicle System Dynamics*, 40(4), 229-270, 2009.
[23] You, S. H., Hahn, J. O., and Lee, H., New adaptive approaches to real-time estimation of vehicle sideslip angle, *Control Engineering Practice*, 17(12), 1367-1379, 2009.
[24] Chen, S., and Chen, F., Simulation-based assessment of vehicle safety behavior under hazardous driving conditions, *Journal of Transportation Engineering*, 136(4), 304-315, 2009.
[25] Dei Li, Y., Liu, W., Li, J., Ma, Z. M., and Zhang, J. C., Simulation of vehicle stability control system using fuzzy PI control method, *Vehicular Electronics and Safety*, IEEE International Conference, IEEE, 2005 (ISBN: 0-7803-9435-6).
[26] Takano, S., and Nagai, M., Dynamics control of large vehicles for rollover prevention, *Vehicle Electronics Conference*, IVEC 2001. Proceedings of the IEEE International, IEEE, 2001 (ISBN: 0-7803-7229-8).
[27] Fancher, P. S., Ervin, R. D., Winkler, C. B., Gillespie, T.D. A factbook of the mechanical properties of the components for single-unit and articulated heavy trucks. Phase I. Final report, Technical Report UMTRI-86-12, University of Michigan Transportation Research Institute, Ann Arbor, MI, USA, 1986.
[28] Hong, D., Hwang, I., Yoon, P, and Huh, K., Development of a vehicle stability control system using brake-by-wire actuators, *Journal of Dynamic Systems, Measurement, and Control*, 130(1), 1-9, 2008.
[29] Haldar, A., and Mahadevan, S., *Probability, Reliability and Statistical Methods in Engineering Design*, John Wiley & Sons, New York, NY, 2000.
[30] Buranathiti, T., Cao, J., Chen, W., Baghdasaryan, L., and Xia, Z.C., Approaches for Model Validation: Methodology and Illustration on a Sheet Metal Flanging Process, *ASME Journal of Manufacturing Science and Engineering*, 126, 2009-2013, 2004.
[31] Hasofer, A. M. and Lind, N. C., An Exact and Invariant First Order Reliability Format, *ASCE Journal of the Engineering Mechanics Division*, 100(1), 111-121, 1974.
[32] Lee, I., Choi, K. K., and Zhao, L., Sampling-Based Stochastic Sensitivity Analysis Using Score Functions for RBDO Problems With Correlated Random Variables, *Journal of Mechanical Design*, 133(2), 1055-1064, 2010.
[33] Ibrahim, S. E. B., and Sayed, T., Developing safety performance functions incorporating reliability-based risk measures, *Accident Analysis & Prevention*, 43(6), 2153-2159, 2011.
[34] Sigbjörnsson, R., and Snæbjörnsson, J. T., Probabilistic assessment of wind related accidents of road vehicles: A reliability approach, *Journal of Wind Engineering and Industrial Aerodynamics*, 74, 1079-1090, 1998.
[35] Snæbjörnsson, J. T., Baker, C. J., and Sigbjörnsson, R., Probabilistic assessment of road vehicle safety in windy environments, *Journal of Wind Engineering and Industrial Aerodynamics*, 95(9), 1445-1462, 2007.
[36] Gustafsson, F., "Slip-based tire-road friction estimation," *Automatica*, 33(6), 1087-1099, 1997.
[37] Harwood, D. W., Torbic, D. J., Richard, K. R., and Glauz, W. D., Review of truck characteristics as factors in roadway design, NCHRP Report 505, Transportation Research Board, Washington, DC, 2003.
[38] Andjus, V., and Maletin, M., Speeds of cars on horizontal curves, *Transportation Research Record: Journal of the Transportation Research Board*, 1612, 42-47, 1998.